Tables I through IV show the liquid phase activity coefficients along with the fugacity coefficients ϕ^0 and vapor pressures p^0 of the pure solutes used in their calculations. The fugacity coefficient ϕ of the solute vapor at infinite dilution in helium gas was also required in the calculations and was taken to be equal to 1. The ϕ^0 values of the esters were obtained from the generalized correlation by Lydersen, Greenkorn, and Hougen (*4*). The ϕ values of the alcohols were calculated based on second virial coefficient data compiled by Dymond and Smith (*2*). The vapor pressures were taken from Jordan's compilation (*3*), and extrapolated by means of a Cox chart where necessary.

The sources and purities of the chemicals used are shown in Table V.

Glossary

F_a volumetric flow rate of elution gas at ambient conditions
K_i equilibrium y_i/x_i for component i
n moles of stationary liquid phase on column packing
p column pressure
p_a ambient pressure
p^0 vapor pressure
R gas constant
t_{R_i} retention time of solute i
t_g retention time of hypothetical "nonabsorbed" gas
T absolute temperature
T_a absolute ambient temperature
V_i liquid molal volume of component i
z_a compressibility factor of elution gas at ambient conditions
γ_i activity coefficient of component i in the liquid phase at T
ϕ_i fugacity coefficient of component i in the elution gas at T and p
ϕ_i^0 fugacity coefficient of pure vapor i at T and p_i^0

Literature Cited

(1) Comanita, V. J., M.S. Thesis, Purdue University, West Lafayette, Ind., Dec 1975.
(2) Dymond, J. H., Smith, E. B., "The Virial Coefficients of Gases", Clarendon Press, Oxford, 1969.
(3) Jordan, T. E., "Vapor Pressure of Organic Compounds", Interscience, New York, N.Y., 1954.
(4) Lydersen, A. L., Greenkorn, R. A., Hougen, O. A., "Generalized Thermodynamic Properties of Pure Fluids", Engineering Experiment Station Report No. 4, University of Wisconsin, Madison, Wis., 1955.
(5) Schreiber, L. B., Eckert, C. A., *Ind. Eng. Chem. Process Des. Dev.*, **10**, 572 (1971).
(6) Turek, E. A., Comanita, V. J., Greenkorn, R. A., Chao, K. C., *J. Chem. Eng. Data*, **21**, 209 (1976).

Received for review March 22, 1976. Accepted July 6, 1976. This work was supported by NSF Grant GK-42051.

Dew Point Study in the Vapor–Liquid Region of the Methane–Carbon Dioxide System

Shuen-Cheng Hwang, Ho-mu Lin,† Patsy S. Chappelear,*‡ and Riki Kobayashi*
Department of Chemical Engineering, William Marsh Rice University, Houston, Texas 77001

The elution technique has been used to study the vapor phase concentration along isotherms in the vapor–liquid region surrounding the vapor–solid region for the methane–carbon dioxide system. Temperatures from −65.00 to −184.00 °F were investigated. The pressure range covered from the three-phase solid–liquid–vapor locus to the critical point or the vapor pressure of methane. Several temperatures matched a previous study in another laboratory in the vapor–solid region. Measurements were intensified near the critical temperature of methane.

There has been a number of studies of the vapor–liquid equilibrium of the methane–carbon dioxide system. However, most of these studies were made at higher temperatures well above the critical temperature of methane, only one investigation included temperatures below the critical temperature of methane.

Both vapor and liquid phases were studied by Arai et al. (*1*) at 59, 32, and −4 °F; by Kaminishi et al. (*6*) at 50, 32, −4, and −40 °F; and by Donnelly and Katz (*4*) at temperatures in the range 29 to −100 °F. Sterner (*10*) measured vapor–liquid equilibria at −90, −95, and −100 °F; however, no critical points were determined. The only investigation which covered the temperature range below methane critical temperature was that by Neumann and Walch (*7*) over the range of −64 to −148 °F.

The solid–liquid–vapor phase behavior of the methane–carbon dioxide system was studied by Pikaar (*8*) and by Davis, Rodewald, and Kurata (*3*). These experimental results have been useful in this investigation for the determination of the triple-point vapor composition locus. The vapor–solid equilibria by Pikaar (*8*) are used for examining the transition between vapor–liquid and vapor–solid regions.

Equipment and Method

In the elution technique, the presaturator and the equilibrium cell are charged with the less volatile component, carbon dioxide in this case. The more volatile component is added to provide the desired system pressure and then eluted through the cell, with a partial recycle to hasten equilibrium. The concentration of the eluted stream is monitored until steady state is achieved.

The main equipment components which were used in the constant flow saturation method consisted of a 410 stainless-steel windowed cell with a pressure rating of 8000 psi, a cryostatic bath, a carrier gas metering pump, and analytic equipment. Extensive details of the equipment and method have been reported earlier (*2*).

The flow chart of the equipment layout is shown in Figure 1.

† Present address, School of Chemical Engineering, Purdue University, West Lafayette, Ind. 47907.
‡ Address correspondence to this author at McDermott Hudson Engineering Corp., Houston, Texas 77036.

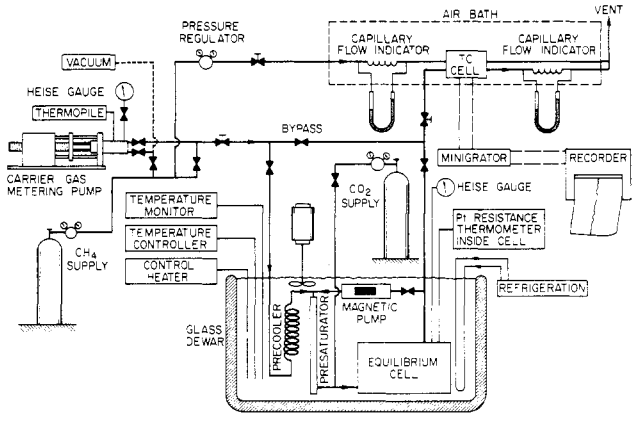

Figure 1. Gas saturation flow system for vapor concentration measurement.

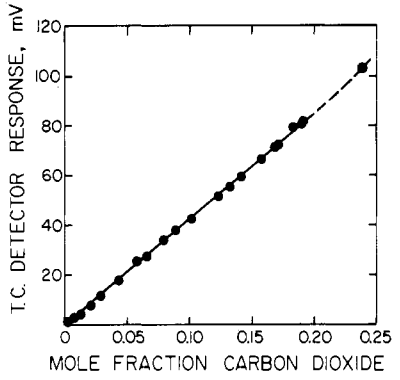

Figure 2. Calibration curve for carbon dioxide in methane.

Pure methane flow is metered by the carrier gas metering pump. The methane flow passes through the by-pass line for a period of time to clear out impurities in the system. The equilibrium cell and presaturator are first evacuated, and then charged with carbon dioxide after the cell and presaturator have been immersed in a stirred cryogenic bath controlled to the desired temperature. After thermal equilibrium is attained, the by-pass line is shut off, and pure methane passes through the precooler to bring the stream temperature to the bath temperature; then it flows through a presaturator made of three 1-ft long sections of $\frac{1}{8}$ in. stainless-steel pipes connected in series, packed with Chromopacks which have been presaturated with carbon dioxide. Finally, the gas stream enters from the bottom of the equilibrium cell, which is two-thirds filled with liquid, initially carbon dioxide.

The effluent dew point gas mixture is expanded to atmospheric pressure and measured continuously by a thermal conductivity cell and recorder. A steady-state condition produces a steady signal on the recorder and a constant cell pressure and pump pressure. After the steady signal voltage on the recorder has been registered, the pure methane flow is again switched to the by-pass line to clear out the mixture and to recheck the baseline. The concentration of the mixture is determined by a calibration curve from the signal difference between the mixture and pure methane.

The detector has been calibrated in a steady flow manner to preserve similarity to the conditions of obtaining the data. A specially designed micropump (*9*) pumps carbon dioxide at a slow rate into the mixing valve, where pure methane is metered by the carrier gas metering pump to mix with the carbon dioxide stream. The temperature of the pump is maintained at 89 °F and the mixing valve at 91 °F. The mixed gas stream then passes into the thermal conductivity cell where a signal is produced by using pure methane from the same cylinder as the reference stream. A pressure transducer was installed at the top of the micropump. When steady state is obtained, the pressure in the carrier gas pump and micropump will stay constant, and the signal from the thermal conductivity cell will also stay at a constant value. The concentration of the mixture can be calculated from the flow rate of both pumps and P-V-T data on each gas (*5, 11*).

Both pumps are kept in thermally controlled (±0.1 °C) air baths to make correct density evaluations and also to eliminate flow fluctuations. Mixtures of various concentrations can be prepared by varying the micropump speed. A mixture stream as dilute as 10^{-7} mole fraction can be prepared. The lower limitation of detection actually is restricted by the sensitivity of the detector. The calibration curve of this detector for the methane–carbon dioxide binary system is shown in Figure 2. The concentration covered ranges from 0.0025 to 0.2 mole fraction of carbon dioxide in methane. The response of the detector is linear up to 0.2 mole fraction. The response curve was fit by linear equation.

Due to experimental limitations, concentrations over 0.2 mole fraction of carbon dioxide cannot be prepared by the combination of the carrier gas metering pump and the micropump. Two primary standard mixtures at 0.16 and 0.24 mole fraction of carbon dioxide prepared by Matheson Gas Products were used for calibration. A curved response was observed for concentration more than 0.2 mole fraction. However, the only data in this region are for the highest isotherm (−65 °F) and one point (400 psia) at the next lower isotherm (−75 °F).

Materials

Ultrahigh purity methane (99.97%) and Coleman Instrument Grade purity carbon dioxide (99.99%) were purchased from Matheson Gas Products. Since the signals from the thermoconductivity detector were obtained by comparing the mixture with the pure methane stream which were originated from the same source, any slight effects on the signals owing to impurity in the methane would be cancelled out.

Experimental Difficulties

Some experimental difficulties were encountered in this investigation. Due to the relative low temperature in the cryostat bath, moisture in the atmosphere will tend to condense and freeze on the connecting rod between the magnetic pump and the pump drive. This causes the magnetic pump to stick. To solve this problem, preheated compressed air was blown on the connecting rod to prevent the condensation.

The second experimental difficulty occurs in the neighborhood of the solid–liquid–gas triple point. In this region, solid carbon dioxide can form and plug the circulating system. In order to prevent the formation of solid, methane was introduced before the carbon dioxide.

Experimental Results

The experimental dew point data for the methane–carbon dioxide binary system are shown in Table I at temperatures from −65 down to −184 °F. Figure 3 is the pressure–concentration plot for isotherms from −65 to −112 °F, with some of the isotherms below −112 °F. The frost-point data from Pikaar (*8*) are also shown in Figure 3 and Figure 4, which gives the pressure–concentration plot for isotherms from −112 down to −184 °F.

The dew point data are shown on a reduced isochoric basis (i.e., the ratio of the system pressure to the isothermal critical pressure) in Figure 5. After preliminary trials, this figure was constructed on the basis of the logarithm of the mole fraction of carbon dioxide vs. the reciprocal of the absolute temperature.

Figure 6 shows the pressure-temperature relations for the

Table I. Dew-Point Data for Methane–Carbon Dioxide System

Pressure, psia	Mole fraction of CO_2	Pressure, psia	Mole Fraction of CO_2	Pressure, psia	Mole fraction of CO_2	Pressure, psia	Mole Fraction of CO_2
T = −65.00 °F = −53.89 °C		T = −75.00 °F = −59.44 °C		T = −114.30 °F = −81.28 °C		T = −115.51 °F = −81.95 °C	
600	0.218	400	0.225	610	0.0444	600	0.043 1
650	0.210	450	0.208	620	0.0401	610	0.033 7
700	0.205	500	0.195	630	0.0362	620	0.039 1
750	0.2023	550	0.185	640	0.0320	630	0.030 0
752	0.2018	600	0.177	641	0.0315	640	0.025 1
800	0.2003	650	0.171	650	0.0268	650	0.019 4
850	0.2019	700	0.168	660	0.0218	660	0.013 9
875	0.205	750	0.167	671	0.0163	670	0.007 93
900	0.211	800	0.168	675	0.0140	671	0.006 61
920	0.221	825	0.170	676	0.0125	672[a]	0.006 78
930	0.226	850	0.175	677[a]	0.0127		
938[a]	0.232	875	0.185				
		880[a]	0.190	T = −116.77 °F = −82.65 °C		T = −130.00 °F = −90.00 °C	
				590	0.041 8	494	0.020 7
T = −81.40 °F = −63.00 °C		T = −94.00 °F = −70.00 °C		600	0.037 6	500	0.017 6
625	0.150	710	0.108	610	0.033 0	504	0.015 3
650	0.148	720	0.107	620	0.028 1	510	0.012 2
675	0.147	730	0.1059	630	0.022 4	515	0.008 84
700	0.1464	740	0.1056	640	0.017 0	520	0.006 18
701	0.1457	750	0.1054	650	0.010 2	525	0.003 33
726	0.1457	760	0.1065	659	0.005 04	528[c]	—
750	0.1456	770	0.110	663	0.002 11		
775	0.1458	773[a]	0.112	665	0.001 08		
800	0.148			666[b]	0.000 00		
810	0.150						
825	0.153			T = −139.43 °F = −95.24 °C		T = −148.00 °F = −100.00 °C	
844[a]	0.163			418	0.014 5	361.7	0.009 32
				427	0.009 24	364.5	0.007 81
T = −104.01 °F = −75.56 °C		T = −112.00 °F = −80.00 °C		438	0.002 95	367.0	0.006 35
680	0.0729	625	0.0512	441.5	0.001 01	370.0	0.004 89
690	0.0709	630	0.0493	445.0[c]	—	372.0	0.004 13
700	0.0689	640	0.0446			375.0	0.002 34
710	0.06643	650	0.0409			377.0	0.001 32
715	0.06636	660	0.0365			377.8[c]	—
720	0.06653	670	0.0323				
723[a]	0.0686	680	0.0282	T = −148.81 °F = −100.45 °C		T = −158.93 °F = −106.07 °C	
		682	0.0272	355.8	0.009 37	294.0	0.005 76
		684	0.0265	356.0	0.009 08	300.0	0.002 41
		685	0.0261	356.2	0.008 94	302.0	0.000 31
		686[a]	0.0264	359.4	0.007 13	302.5[c]	—
				364.5	0.004 33		
				365.8	0.003 50		
				369.8	0.001 07		
				371.8[c]	—		
				T = −184.00 °F = −120.00 °C			
				170.1	0.001 24		
				170.4	0.000 989		
				170.6	0.000 766		
				170.8	0.000 591		
				171.0[c]	—		

[a] Critical. [b] Measured vapor pressure of actual methane cylinder. At this temperature, ref 12 gives 665.8 psia. [c] Vapor pressure of methane from ref 12.

methane–carbon dioxide system at constant mole fraction of methane; i.e., dew point curves. The points shown in both Figures 5 and 6 are smoothed values from the pressure–concentration plots (Figures 3 and 4).

All figures' original size was about 1 m^2. Values shown in Table II were used in the construction of the figures.

Accuracy

Three Heise gauges with ranges of 0–200, 0–500, and 0–2000 psia were used to measure the pressure in the equilibrium cell. The gauges were calibrated by the manufacturer with an accuracy of 0.1% of full scale. The temperature in the equilibrium cell could be controlled to ±0.02 °F. It was measured with a Leeds and Northrup Model 8163-B platinum resistance thermometer which is accurate to at least ±0.01 °C with respect to the IPTS (1968). The overall error in the dew point data is either less than 1% or 0.0001 in mole fraction of carbon dioxide, depending on which is larger.

Comparison of Data

The dew point data for the methane–carbon dioxide system by Neumann and Walch (*7*) and Donnelly and Katz (*4*) are shown in Figures 3 and 4, for comparison with results from this investigation. Figure 3 indicates that the results from previous investigators are somewhat scattered, and, in addition, they qualitatively and quantitatively disagree with this investigation.

The isotherms below the methane critical temperature are

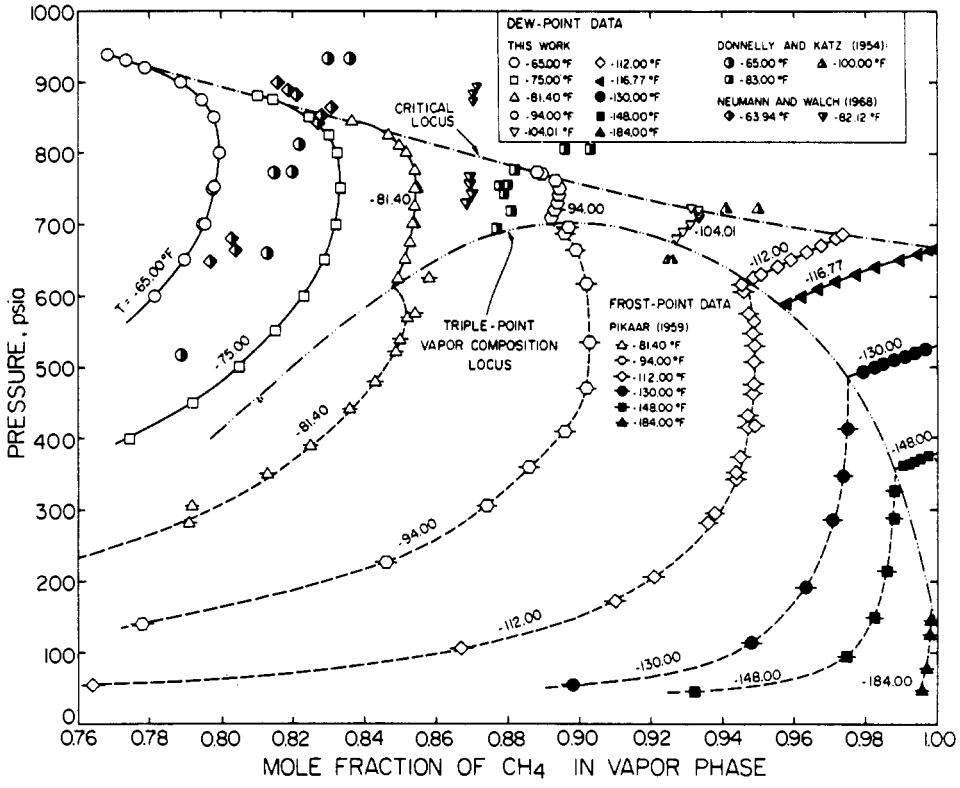

Figure 3. Isothermal dew-point and frost-point data for methane–carbon dioxide.

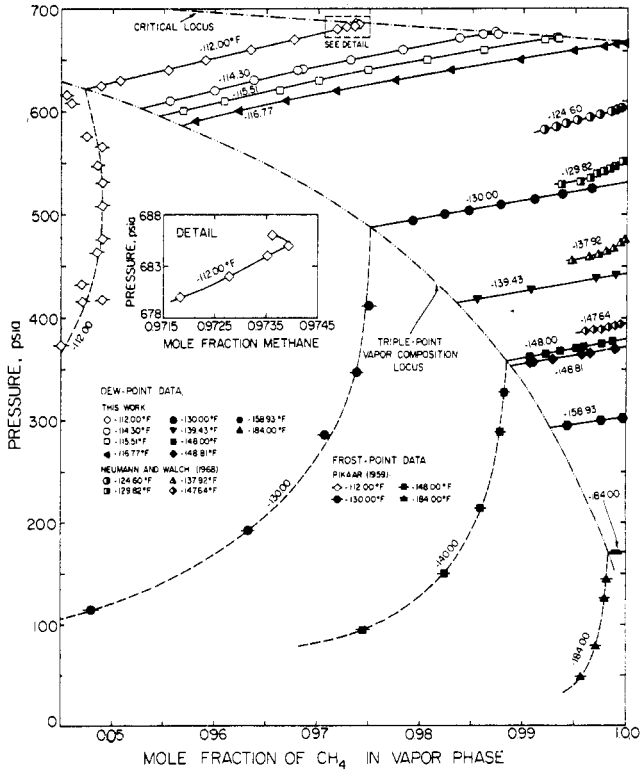

Figure 4. Expanded isothermal dew-point and frost-point data for methane–carbon dioxide from −112 to −184 °F.

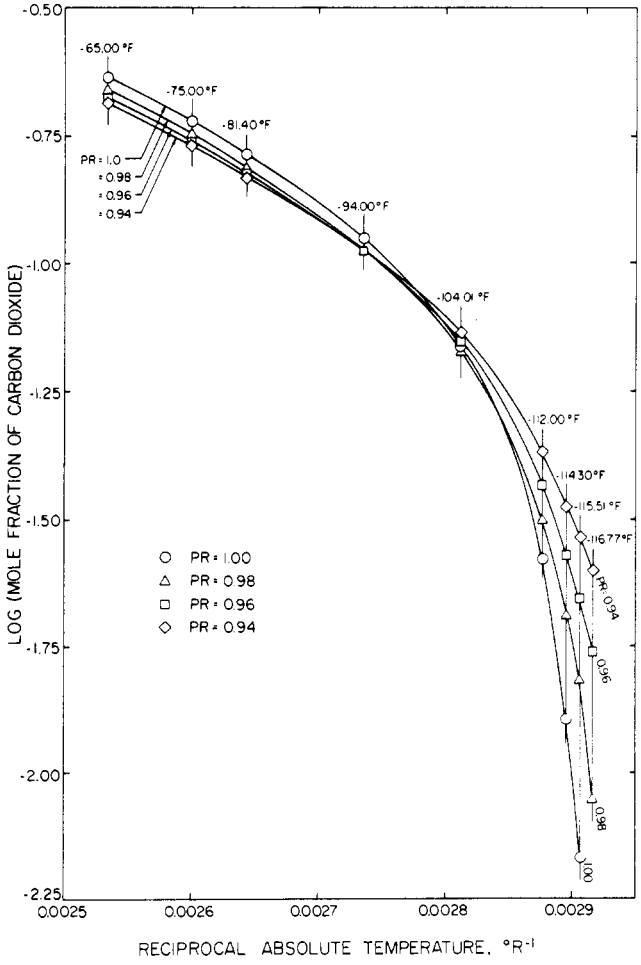

Figure 5. Reduced pressure loci for dew-point data for methane–carbon dioxide system.

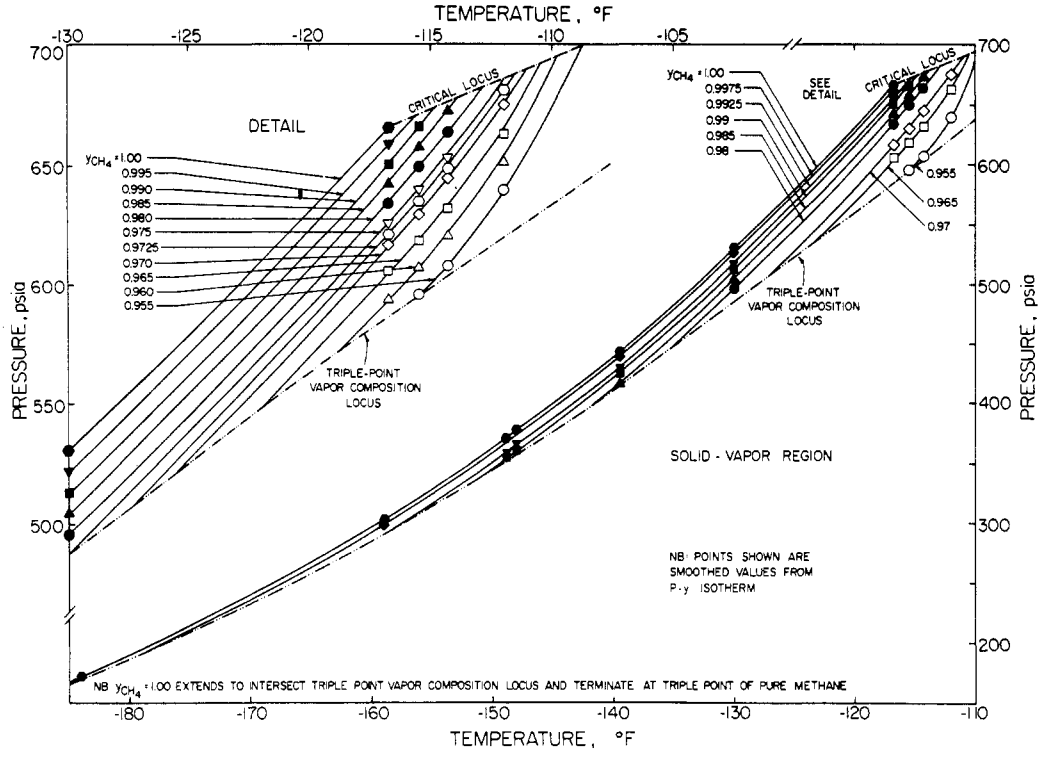

Figure 6. Pressure–temperature relations for methane–carbon dioxide system.

Table II. Triple-Point Vapor Composition Values,[a] Smoothed from Data of Pikaar (*8*) and Davis, Rodewald, and Kurata (*3*)

Temp, °F	Pressure, psia	Mole fraction of CO_2
−81.40	612	0.151 8
−94.00	700	0.108 6
−104.01	676	0.073 7
−112.00	622	0.052 7
−114.30	602	0.047 3
−115.51	595	0.045 4
−116.77	586	0.043 2
−130.00	487.3	0.024 8
−139.43	414.2	0.016 5
−148.00	357.7	0.011 55
−148.81	352.6	0.011 18
−158.93	292.1	0.007 31
−184.00	169.5	0.001 68

[a] Values used in construction of figures.

linear. Similar results were observed by Neumann and Walch (*7*) at −124.60 and −147.64 °F. However, their isotherms at −129.82 and −137.92 °F show a decided curvature. The vapor pressures of methane reported by Neumann and Walch are higher than those by Goodwin (*5*) and Vennix (*12*) by about 30 psia.

It should also be noted that the results reported here have been obtained by two separate investigators. The first study results are the isotherms at −139.43, −148.81, and −158.93 °F; the remainder of the results are from the second study. All results are consistent, as shown in Figures 5 and 6.

Acknowledgment

E.I. du Pont de Nemours and Co. provided the Freon-12 for the cryostat bath fluid. Stephen C. Mraw and Raymond Martin provided extensive assistance with the experimental apparatus.

Literature Cited

(1) Arai, Y., Kaminishi, G., Saito, S., *J. Chem. Eng. Jpn.*, **4** (2), 113 (1971).
(2) Chen, R. J. J., Ruska, W. E. A., Chappelear, P. S., Kobayashi, R., *Adv. Cryog. Eng.*, **18**, 201 (1972).
(3) Davis, J. A., Rodewald, N., Kurata, F., *AIChE J.*, **8**, 537 (1962).
(4) Donnelly, H. G., Katz, D. L., *Ind. Eng. Chem.*, **46** (3), 511 (1954).
(5) Goodwin, R. D., *Natl. Bur. Stand. (U.S.), Tech. Note*, **No. 653** (1974).
(6) Kaminishi, G., Arai, Y., Saito, S., Maeda, S., *J. Chem. Eng. Jpn*, **1** (2), 109 (1968).
(7) Neumann, A., Walch, W., *Chem.-Ing.-Tech.*, **40** (5), 241 (1968).
(8) Pikaar, M. J., Ph.D. Thesis, University of London, London, England (Oct 1959).
(9) Ruska, W. E. A., Carruth, G. F., Kobayashi, R., *Rev. Sci. Instrum.*, **43**, 1331 (1972).
(10) Sterner, C. J., *Adv. Cryog. Eng.*, **6**, 467 (1961).
(11) Van Huff, N. E., Houghton, G., Coull, J., *J. Chem. Eng. Data*, **8**, 336 (1963).
(12) Vennix, A. J., Ph.D. Thesis, William Marsh Rice University, Houston, Texas (April 1966); Vennix, A. J., Leland, T. W., Kobayashi, R., *J. Chem. Eng. Data*, **15**, 238 (1970).

Received for review March 22, 1976. Accepted July 26, 1976. The investigation was supported by the Gas Processors Association, the National Science Foundation, and the American Gas Association.